JOURNAL OF GEOPHYSICAL RESEARCH, VOL. 102, NO. D6, PAGES 6631-6636, MARCH 27, 1997

Nontrivial scaling in the loss of prediction information with aggregation in hourly precipitation occurrences

Alin Cârsteanu and Efi Foufoula-Georgiou

St. Anthony Falls Laboratory, Department of Civil Engineering
University of Minnesota, Minneapolis

Abstract. Predicting the occurrence of rainfall from past patterns of rain/no rain sequences is an issue that has recently regained attention through the application of information theory and dynamical systems, claiming the existence of an underlying complexity of deterministic origin. The present work reports a rather unexpected facet that appeared in the study of hourly precipitation occurrence pattern prediction: the temporal scale invariance of the probability of prediction failure for scales up to the order of magnitude of a storm duration.

1. Prediction From Patterns and the "Chaos Game"

In approaching rainfall time series as the output of a discrete, nonlinear dynamical system, a possibility of prediction becomes available, in that the knowledge about the present state allows us to identify the forward orbit of the system. The "present state" is identified by as many state variables as phase space dimensions the system has. Those in turn can be put in correspondence with pseudo phase space dimensions, as stated by the Takens [1981] embedding theorem, and consequently, the present state of the system can be completely described by a certain number of samples from the past of the variable of interest, if, of course, the iterated function of the system is known. However, in the case of rainfall time series, that iterated function is the result of complicated physics and it practically cannot be derived in a closed form. In such a case, increasing lengths of patterns are used for prediction, by matching them with an existing orbit of sufficient length. The optimal length of utilized patterns can be determined from the point where no essential predictability is gained any more by increasing the pattern length or can be estimated from the dimensionality of the manifold on which the orbit lives in pseudo phase space. That the latter dimensionality can be expected to be reasonably low for atmospheric processes is the conclusion of several authors, notably, *Grassberger* [1986] and *Sharifi et al.* [1990], a fact that suggests that prediction from past patterns is an endeavor worth considering.

Recent work by *Elsner and Tsonis* [1993, 1995] attempts to quantify, for hourly rainfall series, the length of patterns which would lead to a significant predictability. They conclude that the observed precipitation series are neither periodic, nor quasi-periodic, and are definitely more complex than series of independent random variables. The procedure used is known in chaotic dynamics as the "chaos game" [see *Barnsley*, 1988] and consists of determining the allowed versus prohibited transitions between the states of a dynamical system and hereby empirically determining its iteration function. For this purpose, a "state" is described by a discrete sequence (pattern) obtained from a contiguous sample of the process made discrete by applying an indicator function on contiguous disjoint subintervals. In the present work, given the set $S = \{t : R(t) > 0\}$ of instants t of nonzero rainfall R, the indicator function defined on a subset $[t_1, t_2]$

$$I_S([t_1,t_2]) = \begin{cases} 1, & \text{if } \exists t \in [t_1,t_2],\ t \in S \\ 0, & \text{otherwise} \end{cases} \tag{1}$$

is applied. That is to say, two possibilities are taken into account over each subinterval: either it rains at some instant of time (associated value "1") or it does not rain at all (associated value "0"). Other functions taking into account more levels of rainfall intensity may be considered for a more detailed picture. The chaos game procedure comprises finding the patterns of each considered length that do appear in the time series, as opposed to those that do not appear. Notice that the existence/nonexistence of a pattern $\overline{x_1 \ldots x_l}$ tells about the possibility of transition from a state $\overline{x_1 \ldots x_{l-1}}$ to the state $\overline{x_2 \ldots x_l}$ (if pattern length $l-1$ completely describes a state).

Since dimensions analysis of phase space orbits of temporal rainfall intensity signals has hinted to the fact that these orbits might live, as mentioned earlier, on low-dimensional manifolds [*Rodriguez-Iturbe et al.*, 1989; *Sharifi et al.*, 1990; *Tsonis et al.*, 1993], we can expect predictability from relatively short patterns. Notice, however, that in addition to the small number of strong couplings revealed by the dynamical system anal-

Paper number 96JD03530.
0148-0227/97/96JD-03530$09.00

ysis, there exist several weak couplings that make up for the rest of phase space dimensions of fully developed, two-fluid turbulence with heat exchange in the atmosphere. For the purpose of prediction, we consider these weak couplings in the form of noise and adopt a probabilistic rather than deterministic approach to the transitions between states in the chaos game procedure. Specifically, we adopt the approach described in the next section.

2. Probabilities of Prediction Success and Prediction Failure

Let us denote by $\mathcal{P}[\overline{x_1 \dots x_l}]$ the probability of occurrence of the 0–1 pattern $\overline{x_1 \dots x_l}$. Obviously,

$$\mathcal{P}[\overline{x_1 \dots x_l 0}] = \mathcal{P}[0|\overline{x_1 \dots x_l}]\mathcal{P}[\overline{x_1 \dots x_l}]$$
$$\mathcal{P}[\overline{x_1 \dots x_l 1}] = \mathcal{P}[1|\overline{x_1 \dots x_l}]\mathcal{P}[\overline{x_1 \dots x_l}] = 1 - \mathcal{P}[\overline{x_1 \dots x_l 0}]$$

We estimate these probabilities from our data by

$$\widehat{\mathcal{P}}[\overline{x_1 \dots x_l 0}] = \frac{N[\overline{x_1 \dots x_l 0}]}{L - l + 1} \tag{2}$$

where $N[\cdot]$ is the number of occurrences of the sequence in the argument within a series of total length L. A similar estimator is used for $\mathcal{P}[\overline{x_1 \dots x_l 1}]$. We call "probability of prediction success" the maximal value of $\mathcal{P}[0|\overline{x_1 \dots x_l}]$ and $\mathcal{P}[1|\overline{x_1 \dots x_l}]$, i.e.,

$$\mathcal{P}[\text{success}|\overline{x_1 \dots x_l}] = \max\{\mathcal{P}[0|\overline{x_1 \dots x_l}], 1 - \mathcal{P}[0|\overline{x_1 \dots x_l}]\}, \tag{3}$$

which is the probability of correctly predicting a rain/no rain situation in the next sample, given the pattern $\overline{x_1 \dots x_l}$. This probability is computed for all sequences of length l that appear in the series, and an average value over all these sequences of length l is interpreted as our "average probability of prediction success" $\overline{\mathcal{P}}[\text{success}|\overline{x_1 \dots x_l}]$, given a past sample sequence of length l. The probabilities of prediction success are valued between 0.5 and 1 and are nondecreasing with pattern length. Their complements, the "probabilities of prediction failure," are therefore valued between 0 and 0.5 and nonincreasing with pattern length. The ranges are trivially valid for the average probabilities of prediction success/failure too, whereas the monotonicity property holds via conditional probabilities. The estimators $\widehat{\mathcal{P}}$ will show the same statistical properties for a sufficiently long series. One may want to linearly rescale the above probabilities between 0 and 1 in order to obtain normalized measures of failures and successes, respectively. The standard deviation of $\mathcal{P}[\text{success}|\overline{x_1 \dots x_l}]$ across sequences of length l is a measure of the spread of the goodness of our prediction. Most importantly, a significant increase of the standard deviation with pattern length is an alarm signal that a pattern length has been reached, where too many of the patterns appear just a few times, rendering the calculated average less reliable. Figure 1 depicts the increase in standard deviation that accompanies the apparent (and therefore misleading) increase in average prediction success at large pattern lengths.

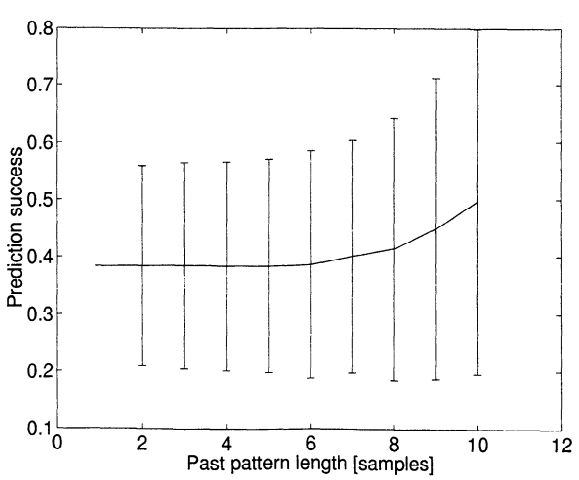

Figure 1. Estimated average probability of prediction success plotted with 1 standard deviation above and below it, as a function of the pattern length used in prediction, for a 6-year daily precipitation occurrence series from Minneapolis, Minnesota.

3. Behavior of Prediction Success in Temporal Rainfall Occurrence Series From Over the United States

The average probability of prediction success (also called here "prediction success" for simplicity) as a function of pattern length at 12 U.S. locations has been estimated for samples aggregated to intervals of 1 hour (basic available sampling interval), and 2, 6, 12 and 24 hours. These prediction successes have been plotted in Figure 2 as a function of past pattern length and for two aggregation intervals, hourly (Figure 2, top) and 6 hours (Figure 2, bottom) for the 12 U.S. locations. As can be seen from Figure 2, the behavior of prediction success is quite similar for both the hourly and six-hour aggregated series; they both show a well-defined saturation level starting at the pattern length 1. Similar results (not displayed here) are found for aggregation intervals of 2, 12, and 24 hours. Thus, overall, it is seen that irrespectively of the aggregation level, no substantial gain in prediction success of rainfall occurrence is obtained by increasing pattern length to more than one aggregation interval. However, the saturation level of prediction success depends on the aggregation level, and, as expected, it decreases as the aggregation level increases. (We note that for rainfall which is here measured as an occurrence/nonoccurrence process over a specified interval, aggregation level is equivalent to what is usually referred to as sampling interval.)

The most interesting property emerging from this analysis is a power law scaling of the saturation values of prediction failure with aggregation. In a log-log repre-

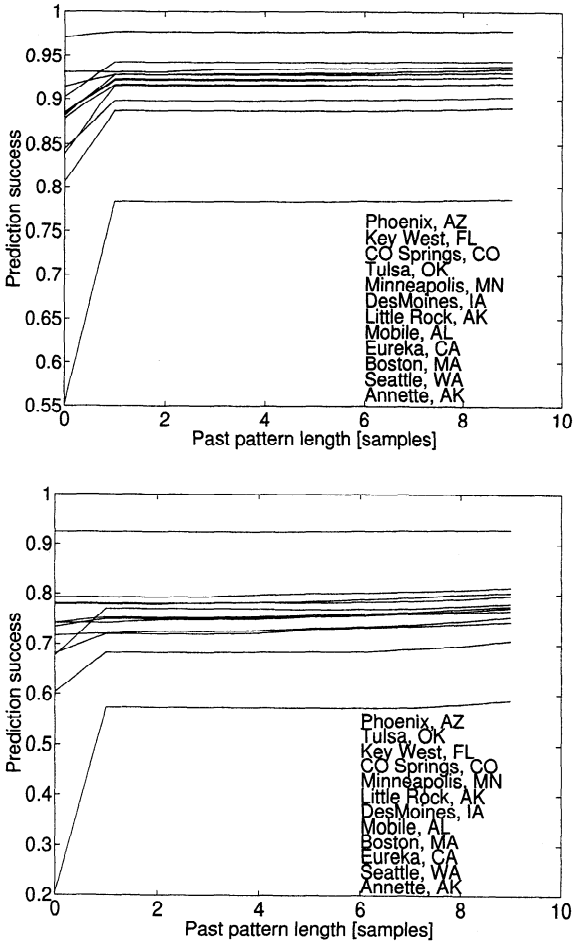

Figure 2. Prediction success of (top) hourly and (bottom) 6-hour precipitation occurrence series from 12 U.S. locations, as a function of the pattern length used in the prediction. Locations are listed in decreasing order of intersection with the ordinate. All locations show a saturation level after pattern length 1.

sentation of prediction failure against aggregation level, good scaling can be observed for small enough values of prediction failure, i.e., for small enough percentages of rainy samples. For most stations, scaling would hold throughout sampling lengths of 24 hours (Figure 3). In the places with the most frequent precipitation, however (Annette, Alaska; Seattle, Washington) a scaling break has to occur. The scaling exponents at the 10 locations which show good scaling (including Phoenix, Arizona, which has a sensibly lower precipitation occurrence rate) are quite close to each other, having values of 0.63-0.69; the (slight) exception is Eureka, California with a value of 0.5.

Notice that for "blind" prediction (i.e., based only on rain/no rain statistics, without any knowledge of the immediate past), the prediction failure scales with aggregation level by definition with an exponent equal to $1 - D_c$, where D_c is the capacity dimension of the set generated by the points of nonzero precipitation on the time line. D_c is defined as $\limsup_{\epsilon \to 0}(-\log N_\epsilon[1]/\log \epsilon)$, where $N_\epsilon[1]$ is the number of disjoint subintervals of length ϵ whose indicator function is equal to 1. From here we have that $1-D_c = 1+\limsup_{\epsilon \to 0}(\log N_\epsilon[1]/\log \epsilon) = \limsup_{\epsilon \to 0}(\log \mathcal{P}_\epsilon[1]/\log \epsilon)$, where the index ϵ refers to the sampling interval length. This can be verified also from the analyzed data by plotting in log-log scale the values of the prediction failure at past pattern length zero (see Figure 3, top) versus aggregation level. The remarkable fact in these rainfall time series is that prediction failure also scales for subsequent, increasing pattern lengths. This kind of scaling found in the values of prediction failure leads us to a different choice of model than would result from taking into account the short-memory feature only. A 0–1 Markov process, by having a memory of one time step, emulates the saturation of prediction success after pattern length = 1 (as seen in Figure 1), to some degree (see Figure 4, top).

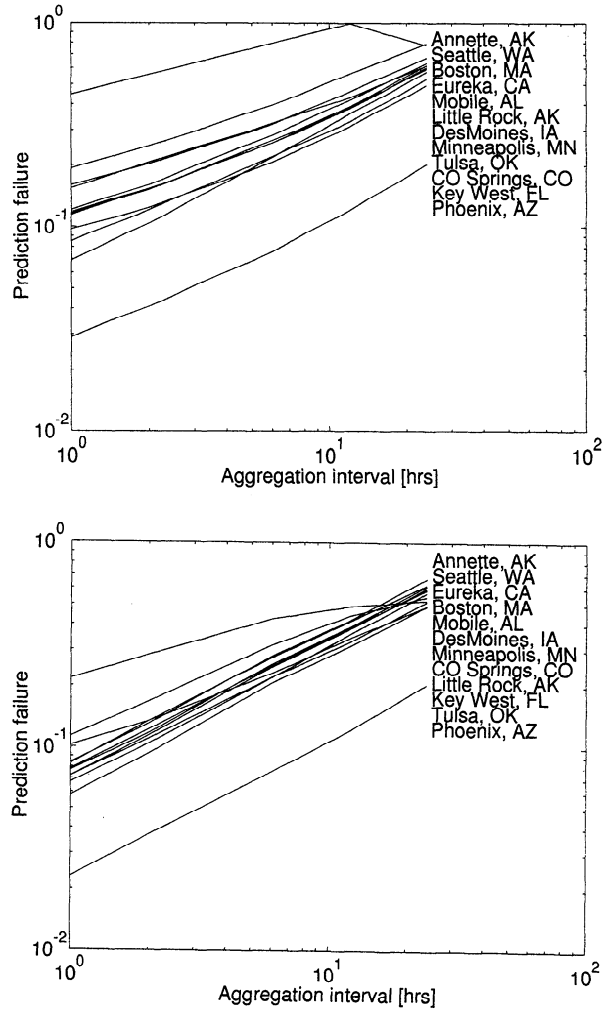

Figure 3. Loss of prediction success through aggregation of hourly precipitation occurrence series from 12 U.S. locations. The past pattern length is equal to (top) zero and (bottom) one sample. Locations are listed in decreasing order of intersection with the ordinate. With the exception of Annette, Alaska, all locations show almost perfect linear fits, with correlation coefficients above 0.99.

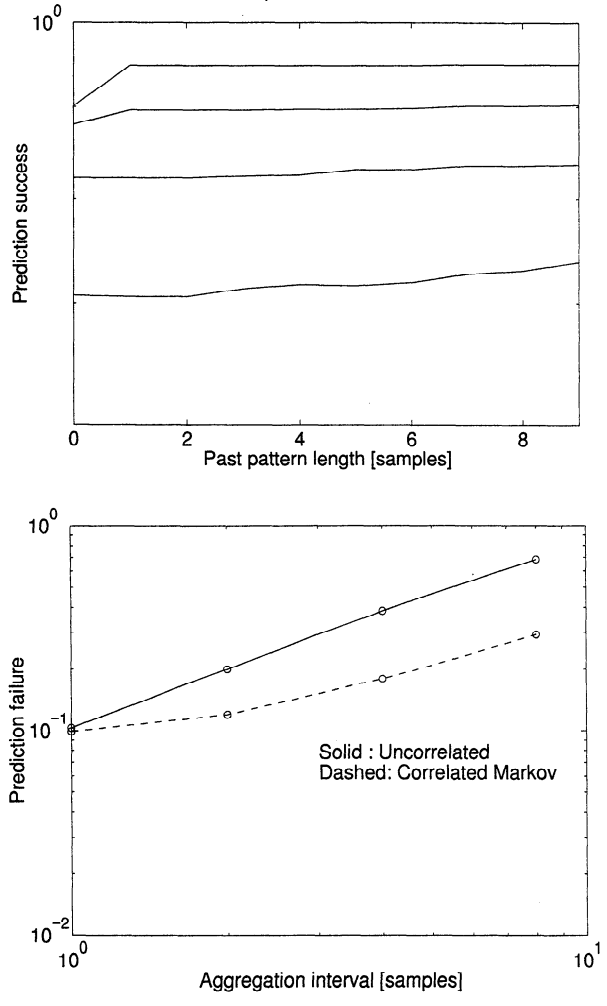

Figure 4. Behavior of prediction failure in a Markov series with parameters emulating the rainfall occurrence series: average = 0.05, lag-1 autocorrelation = 0.7. (top) Behavior of prediction success at pattern lengths 0,...,9 for aggregation intervals 1 (bottom line), 2, 4, and 8 (top line). (bottom) Scaling of prediction failure against aggregation interval for unit pattern length. Notice that in the uncorrelated case, the slope of the line is approximately 1, whereas in the correlated case, scaling does not occur. However, since with aggregation, the initial exponentially decaying correlation disappears, for higher aggregation lengths, we see a tendency to align to the same unit slope.

However, such a Markov series shows either no scaling or a trivial nonfractal scaling (for correlated and uncorrelated Markov series, respectively) in prediction failure against aggregation, with an integer scaling exponent equal to unity (see Figure 4, bottom). Therefore, as the values of prediction success or failure at different pattern lengths are the result of an intricate tree of conditional probabilities, the scaling of these resulting values makes a statement about preserving an internal structure of the series under aggregation. This distinct internal structure of rainfall and its deviation from Markovian (short memory) models prompted us to investigate the behavior of prediction failure under aggregation in a simple, self-similar (long memory) model and see if that compares better to the rainfall structure. The models chosen for study are the random monofractal cascades ("random Cantor sets"). These models are theoretically shown in the next section to exhibit the type of scaling in prediction failure observed in the precipitation time series, i.e., for all pattern lengths. Also, the scaling exponents in these models can be readily chosen to match those observed in the rainfall process.

4. Behavior of Prediction Success in Random Monofractal Cascades

To understand the behavior of temporal rainfall pattern predictability obtained at different locations over the United States, we take a look at how the pattern predictability behaves in a random monofractal cascade. From examining a few simulated cascades, the value of $1 - D_c$ for the scaling exponent of prediction failure, as found empirically in the precipitation series for different pattern lengths, is also matched with several random Cantor sets (Figure 5). This empirical finding prompts us to theoretically study random Cantor sets, such that we can more rigorously conclude whether self-similar models can emulate the pattern predictability behavior of temporal rainfall. We prove here that the probability of prediction failure, as defined in section 2, scales with aggregation time with an exponent equal to $1 - D_c$ for that cascade. Let us first have a look at a two-thirds random Cantor set C in order to keep a general proof from being overly abstract. We consider the Cantor set within the unit interval and its indicator function I_C defined as in (1). By splitting the unit interval subsequently in $3^0 = 1$, $3^1 = 3$, $3^2 = 9$, ..., 3^n equal subintervals, we essentially recover from our indicator function the (monofractal) multiplicative ternary cascade that generated the Cantor set.

Our pattern prediction procedure looks at patterns created by the values of the indicator function on consecutive subintervals of length 3^{-n} (at the nth splitting "level" of the cascade). We denote $\mathcal{P}^{(n)}[\overline{10}]$ the probability of a sequence $\overline{ab}$ to be $\overline{10}$, at the nth level. We analyze first (as we do for rainfall) the probability of prediction failure from past patterns of length 1 by looking at realizations of patterns of length 2, as described in the appendix. The probability of success for length-1 pattern prediction for this type of Cantor set becomes $\mathcal{P}^{(n)}[\overline{00}] + \mathcal{P}^{(n)}[\overline{10}] = \mathcal{P}^{(n)}[0]$, whereas the probability of failure is $\mathcal{P}^{(n)}[\overline{01}] + \mathcal{P}^{(n)}[\overline{11}] = \mathcal{P}^{(n)}[1]$. We observe that these are exactly the probabilities for 0-length ("blind") prediction, a fact that creates the leveling of success (or failure) probability against pattern length, as found in different places in the rainfall time series analysis. The scaling is, in this particular case, obvious, since the scaling exponent of $\mathcal{P}^{(n)}[1]$ is $1 - D_c$, as shown in the previous section.

Let us now look at the general case of an (m, k) self-

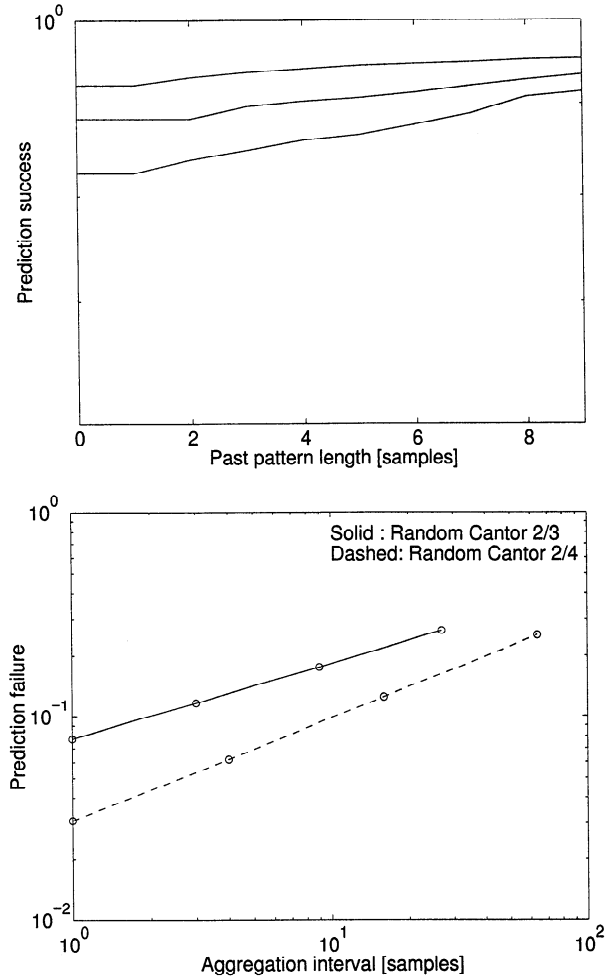

Figure 5. Loss of prediction success through aggregation of "hourly" data drawn from random Cantor sets. (top) Behavior of prediction success at pattern lengths 0,...,9 for aggregation interval = 1 (bottom line), 2 (middle line), and 4 (top line) in a random "two-thirds" Cantor set. (bottom) Scaling of prediction failure against aggregation interval for pattern length equal to one sample. The solid line is for a random two-thirds Cantor set (slope equals $1 - \ln 2/\ln 3 \approx 0.37$), and the dashed line is for a random two-quarters Cantor set (slope equals $1 - \ln 2/\ln 4 = 1/2$).

similar set (generated by a random multinomial k-ary multiplicative cascade, with m weights $= 1$ and $k - m$ weights $= 0$). From the appendix, we see how $\mathcal{P}^{(n)}[\overline{11}]$ and $\mathcal{P}^{(n)}[\overline{10}]$ can be written in terms of $\mathcal{P}^{(n-1)}$ (see (A1) and (A2)), and thus, in the general case, take the form:

$$\mathcal{P}^{(n)}[\overline{1x}] \equiv \mathcal{P}^{(n)}[x|1]\mathcal{P}^{(n)}[1] = \frac{\mathcal{P}^{(n-1)}[1]}{3} \times \frac{(\ldots)+(\ldots)+\cdots+(\ldots)}{\binom{k}{m}}, \quad (4)$$

where $\binom{k}{m}$ is the number of permutations resulting from all linear combinations of $\mathcal{P}^{(n)}[\overline{10}]$ and $\mathcal{P}^{(n)}[\overline{11}]$, and the parentheses on the right-hand side contain constants and terms in $\mathcal{P}^{(n-1)}$. Since there are only pairs of two multiplicative terms in the recursive equations of $\mathcal{P}^{(n)}[\overline{1x}]$, the equivalents of (A4) and (A5) in the appendix will necessarily be of the form

$$\mathcal{P}^{(n)}[x|1] = C + B\alpha^n + A\beta^n. \quad (5)$$

Since $\mathcal{P}^{(n)}[x|1] \leq 1$, we have that $\alpha, \beta < 1$. Denote then $\lim_{n\to\infty} \mathcal{P}^{(n)}[0|1] = C_0$ and $\lim_{n\to\infty} \mathcal{P}^{(n)}[1|1] = C_1$. Since $C_1 + C_0 = 1$, they cannot both be zero and therefore $\max(C_1, C_0) > 0$. This, in turn, implies two possibilities.

1. $C_1 > C_0$. Probability of success $= \mathcal{P}^{(n)}[\overline{00}] + \mathcal{P}^{(n)}[\overline{11}] > \mathcal{P}^{(n)}[0]$, so the probability of success increases at this point with pattern length; probability of failure $= \mathcal{P}^{(n)}[\overline{01}] + \mathcal{P}^{(n)}[\overline{10}] \to 2C_0\mathcal{P}^{(n)}[1] < \mathcal{P}^{(n)}[1]$. Also, since $\mathcal{P}^{(n)}[0] > 0$ and from above, $0 < \mathcal{P}^{(n)}[\overline{11}] < \mathcal{P}^{(n)}[1]$, we have $\mathcal{P}^{(n)}[\overline{10}] > 0 \Longrightarrow C_0 > 0$. Since $\lim_{n\to\infty}(\mathcal{P}^{(n)}[\overline{10}]/\mathcal{P}^{(n)}[1]) = \lim_{n\to\infty} \mathcal{P}^{(n)}[0|1] = C_0 > 0$ (that is, in the limit, there is a strictly positive ratio between $\mathcal{P}^{(n)}[\overline{10}]$ and $\mathcal{P}^{(n)}[1]$) we conclude that $\mathcal{P}^{(n)}[\overline{10}]$ scales as $\mathcal{P}^{(n)}[1]$.

2. $C_0 \geq C_1$. Probability of success $= \mathcal{P}^{(n)}[\overline{00}] + \mathcal{P}^{(n)}[\overline{10}] = \mathcal{P}^{(n)}[0]$, so the probability of success is leveling off at this point as a function of pattern length; probability of failure $= \mathcal{P}^{(n)}[\overline{01}] + \mathcal{P}^{(n)}[\overline{11}] = \mathcal{P}^{(n)}[1]$, which scales, by definition, with the capacity dimension.

This concludes the proof that, indeed, for random monofractal cascades, the probability of prediction failure at pattern length 1 scales as $\mathcal{P}^{(n)}[1]$. Moreover, the same argument can be inductively repeated for higher pattern lengths, by simply replacing $\mathcal{P}^{(n)}[1]$ with $\mathcal{P}^{(n)}[\overline{10}] + \mathcal{P}^{(n)}[\overline{01}] + \mathcal{P}^{(n)}[\overline{11}]$ and $\mathcal{P}^{(n)}[0]$ with $\mathcal{P}^{(n)}[\overline{00}]$, and so forth.

5. Conclusions

We have shown that prediction failure from past patterns of varying length in temporal rainfall occurrence series from over the United States scales against aggregation length with an exponent that was found by estimation to be equal to $1-D_c$, with D_c being the capacity dimension of the rainfall occurrence series. At the same time, we have given a theoretical proof that this is also the case for random monofractal cascade models. We therefore conclude that in view of these findings, multiplicative (random or structured) monofractal cascades make a more appropriate model for temporal rainfall occurrence, in terms of capturing the predictability structure of rainfall, than a Markovian model, which would otherwise be the first choice in view of the short-term memory found in the temporal rainfall series, but which is herein shown not to resemble the predictability structure of rain. Let us also point out that introducing a dependence structure within the random Cantor sets [see *Cârsteanu and Foufoula-Georgiou*, 1996] captures another degree of freedom of cascades, making it thus possible for the cascade model to match the different

prediction powers of patterns of the same length and the pattern lengths at which the leveling of prediction success occurs for the process. However, this is a subject in itself, beyond the scope of this article.

Appendix

It is shown here how we obtain the probabilities $\mathcal{P}^{(n)}$ of occurrence of each length-2 pattern at the nth stage of construction of a ternary random multiplicative cascade. We obtain the probabilities of transition from length-1 past patterns by analyzing realizations of all possible patterns of length 2 that occur at one stage (passing from level $n-1$ to level n):

1 1 0 or ●●○
0 1 1 or ○●●
1 0 1 or ●○●

We write from the above

$$\begin{aligned}\mathcal{P}^{(n)}[\overline{11}] &\equiv \mathcal{P}^{(n)}[1|1]\mathcal{P}^{(n)}[1] \\ &= \frac{\mathcal{P}^{(n-1)}[1]}{3} \times \frac{2\left(1+\frac{1}{3}\mathcal{P}^{(n-1)}[1|1]\right)+\frac{2}{3}\mathcal{P}^{(n-1)}[1|1]}{3} \\ &= \frac{\mathcal{P}^{(n-1)}[1]}{9}\left(2+\tfrac{4}{3}\mathcal{P}^{(n-1)}[1|1]\right) \\ &\equiv \tfrac{2}{9}\left(\mathcal{P}^{(n-1)}[1]+\tfrac{2}{3}\mathcal{P}^{(n-1)}[\overline{11}]\right) \qquad \text{(A1)}\end{aligned}$$

$$\begin{aligned}\mathcal{P}^{(n)}[\overline{10}] &\equiv \mathcal{P}^{(n)}[0|1]\mathcal{P}^{(n)}[1] \\ &= \mathcal{P}^{(n)}[\overline{01}] \equiv \mathcal{P}^{(n)}[1|0]\mathcal{P}^{(n)}[0] \\ &= \frac{\mathcal{P}^{(n-1)}[1]}{9}\left(2+\tfrac{2}{3}\mathcal{P}^{(n-1)}[1|1]+2\mathcal{P}^{(n-1)}[0|1]\right) \\ &\equiv \tfrac{2}{9}\left(\mathcal{P}^{(n-1)}[1]+\tfrac{1}{3}\mathcal{P}^{(n-1)}[\overline{11}]+\mathcal{P}^{(n-1)}[\overline{10}]\right) \qquad \text{(A2)}\end{aligned}$$

$$\begin{aligned}\mathcal{P}^{(n)}[\overline{00}] &\equiv \mathcal{P}^{(n)}[0|0]\mathcal{P}^{(n)}[0] \\ &\equiv 1-\mathcal{P}^{(n)}[\overline{11}]-\mathcal{P}^{(n)}[\overline{10}]-\mathcal{P}^{(n)}[\overline{01}] \qquad \text{(A3)}\end{aligned}$$

With $\mathcal{P}^{(n)}[1] = (2/3)^n$ and $\mathcal{P}^{(n)}[0] = 1-(2/3)^n$, we obtain

$$\begin{aligned}\mathcal{P}^{(n)}[1|1] &= \frac{3}{7}+\frac{9}{28}\left(\frac{2}{9}\right)^n \\ \Longrightarrow \mathcal{P}^{(n)}[\overline{11}] &= \left(\tfrac{2}{3}\right)^n\left[\tfrac{3}{7}+\tfrac{9}{28}\left(\tfrac{2}{9}\right)^n\right] \qquad \text{(A4)}\end{aligned}$$

$$\begin{aligned}\mathcal{P}^{(n)}[0|1] &= \frac{4}{7}-\frac{9}{28}\left(\frac{2}{9}\right)^n \\ \Longrightarrow \mathcal{P}^{(n)}[\overline{10}] &= \left(\tfrac{2}{3}\right)^n\left(\tfrac{4}{7}-\tfrac{9}{28}\left(\tfrac{2}{9}\right)^n\right). \qquad \text{(A5)}\end{aligned}$$

Since for sufficiently large n, we have $\mathcal{P}^{(n)}[\overline{10}] > \mathcal{P}^{(n)}[\overline{11}]$ and, of course, $\mathcal{P}^{(n)}[\overline{00}] > \mathcal{P}^{(n)}[\overline{01}]$, the probability of success for length-1 pattern prediction for this type of Cantor set becomes $\mathcal{P}^{(n)}[\overline{00}]+\mathcal{P}^{(n)}[\overline{10}] = \mathcal{P}^{(n)}[0]$, whereas the probability of failure is $\mathcal{P}^{(n)}[\overline{01}]+\mathcal{P}^{(n)}[\overline{11}] = \mathcal{P}^{(n)}[1]$.

Acknowledgments. The authors hereby acknowledge the support of NSF (grant EAR-9117866), NASA (grant NAG5-2108), and NOAA (grant NA46GP0486).

References

Barnsley, M., *Fractals Everywhere*, Academic, San Diego, Calif., 1988.

Cârsteanu, A., and E. Foufoula-Georgiou, Assessing dependence among weights in a multiplicative cascade model of temporal rainfall, *J. Geophys. Res., 101*(D21), 26,363, 1996.

Elsner, J.B., and A.A. Tsonis, Complexity and predictability of hourly precipitation, *J. Atmos. Sci., 50*(3), 400, 1993.

Elsner, J.B., and A.A. Tsonis, Estimating the complexity and predictability of hourly precipitation, paper presented at the Fifth International Conference on Precipitation: Space-Time Variability and Dynamics of Rainfall, sponsored by NSF, NASA, NOAA, EC, Elounda, Crete, Greece, June 1995.

Grassberger, P., Do climatic attractors exist?, *Nature, 323*, 609, 1986.

Rodriguez-Iturbe, I., B. Febres de Power, M.B. Sharifi, and K.P. Georgakakos, Chaos in rainfall, *Water Resour. Res., 25*(7), 1667, 1989.

Sharifi, M.B., K.P. Georgakakos, and I. Rodriguez-Iturbe, Evidence of deterministic chaos in the pulse of storm rainfall, *J. Atmos. Sci., 47*(7), 888, 1990.

Takens, F., Detecting strange attractors in turbulence, in *Lecture Notes in Mathematics*, vol. 898, edited by A. Dold and B. Eckmann, p. 366, Springer-Verlag, New York, 1981.

Tsonis, A.A., J.B. Elsner, and K.P. Georgakakos, Estimating the dimension of weather and climate attractors: Important issues on the procedure and interpretation, *J. Atmos. Sci., 50*(15), 2249, 1993.

A. Cârsteanu and E. Foufoula-Georgiou, St. Anthony Falls Laboratory, Department of Civil Engineering, University of Minnesota, Mississippi River at Third Avenue SE, Minneapolis, MN 55414. (e-mail: alin@mykonos.safhl.umn.edu; efi@mykonos.safhl.umn.edu)

(Received October 16, 1996; accepted October 16, 1996.)